

Capacity for Electromagnetic Information Theory

Zhongzhichao Wan, Jieao Zhu, Zijian Zhang, and Linglong Dai

Abstract—Traditional channel capacity based on one-dimensional time domain mismatches the four-dimensional electromagnetic fields, thus it cannot fully exploit the information in the spatial dimensions. Therefore, electromagnetic information theory based on the four-dimensional electromagnetic fields becomes necessary to reveal the fundamental theoretical capacity bound of the communication systems. Existing works on electromagnetic information theory focused on deterministic signals and degrees of freedom, which were unable to derive the capacity due to the lack of entropy definition. In this paper, we first model the communication between two continuous regions by random field. Then, we analyze a special case with parallel linear source and destination to derive the capacity bound. Specifically, for parallel infinite-length source and destination, we analyze the mutual information by spatial spectral density and derive the best current distribution on the source to achieve the maximum mutual information, i.e., the capacity. Then, we analyze the scenario with infinite-length source and finite-length destination. We use Mercer expansion to derive the mutual information between the source and the destination. Finally, for a practical model with finite-length source and destination, we analyze its Mercer expansion and reveal its connection with the infinite-length case. The capacity we analyzed reveals the theoretical limit of the communication rate between two continuous regions.

Index Terms—Electromagnetic information theory (EIT), capacity analysis, spatial correlation, spatial spectral density (SSD).

I. INTRODUCTION

Wireless communication systems usually utilize four-dimensional electromagnetic fields, including one time dimension and three spatial dimensions, for information exchange. However, the classical Shannon information theory analyzes the capacity of one-dimensional signals between source and destination only in the time domain, which mismatches the four-dimensional electromagnetic fields of actual communication systems [1]. The modern multiple-input multiple-output (MIMO) technology is, intrinsically, an attempt to utilize the extra information contained in the remained three spatial dimensions [2]. Although the MIMO technology tries to capture the information from the spatial dimensions, due to the simple discretization of the continuous spatial dimensions, it fails to fully explore the spatial information [3]. Therefore, we should restore to the continuous four-dimensional electromagnetic fields to analyze the ultimate performance limit of arbitrary

All authors are with Beijing National Research Center for Information Science and Technology (BNRist) as well as the Department of Electronic Engineering, Tsinghua University, Beijing 100084, China (E-mails: {wzzc20, zja21, zhangj20}@mails.tsinghua.edu.cn; dail1@tsinghua.edu.cn).

This work was supported in part by the National Key Research and Development Program of China (Grant No. 2020YFB1807201), in part by the National Natural Science Foundation of China (Grant No. 62031019), and in part by the European Commission through the H2020-MSCA-ITN META WIRELESS Research Project under Grant 956256.

communication system, which leads to the research of the electromagnetic information theory (EIT) [4].

For EIT, one approach to analyze the ultimate performance limit is based on the Kolmogorov ϵ -capacity. Different from the Shannon capacity which is the maximum number of bits that can be transmitted through a given channel, the Kolmogorov ϵ -capacity is the minimum number of bits required to reconstruct a particular message. An optimization method was established for the calculation of Kolmogorov ϵ -capacity in [5]. This method relied on simulations, so it failed to provide theoretical solutions to the degrees of freedom (DoF) and capacity in general cases.

Another approach is called the spatial bandwidth [6], based on which the DoF can be theoretically derived for EIT. The spatial bandwidth is similar to the widely-used bandwidth in time-frequency domain. The bandwidth characterizes the band-limited feature in the frequency domain [7], and can be utilized to derive the DoF in unit time when the entire observed time window is long enough [8]. Similarly, the spatial bandwidth depicts the band-limited feature in the wavenumber domain, which is the Fourier transform of the space domain, and can be utilized to derive the DoF in unit space when the occupied space is large enough. The spatial bandwidth of scattered fields was rigorously derived in [9]. It was shown that for a time-harmonic model bounded in a sphere, the spatial bandwidth is linear with the frequency and the radius of the sphere. Further works extended the time-harmonic model, which is on single frequency point, to a more general frequency band-limited model and analyzed the DoF in [10]. Unfortunately, all above works based on spatial bandwidth provide the DoF in unit space only when the occupied space of the destination is large enough. By contrast, for practical communication systems in a limited space, the spatial bandwidth method becomes inaccurate.

For the practical communication system in a limited space, several works utilized the expansion on orthogonal basis to derive the DoF for EIT. For example, inspired by the orthogonal-frequency division-multiplexing (OFDM), [3] designed a set of bases to expand the Green function to derive the DoF between two parallel finite-length linear antennas. Moreover, for the scenario when the two finite-length linear antennas had an intersection angle, a heuristic method was proposed to construct the bases to derive the DoF in [11]. Furthermore, [12] proposed an optimization method that can maximize the DoF for general scenarios. These works provided useful methods for analyzing the DoF for EIT. However, they heavily relied on the assumption of deterministic signals, thus being unable to derive the capacity.

Different from existing works on DoF which rely on the assumption of deterministic signals, in this paper, we analyze

the capacity based on the random field theory¹. The capacity we analyzed reveals the theoretical limit of the communication rate between two continuous regions. Specifically, the contributions of this paper are summarized as follows.

- We first develop the system model of the communication between two four-dimensional continuous regions. We use random field instead of the traditional deterministic signals to capture the statistical characteristics of the electromagnetic field of the communication system. The mutual information between the source and the destination is derived in a limit form by sampling on the continuous destination region. The best covariance matrix of the sampling points can be derived by the Kuhn-Tucker conditions to achieve the maximum mutual information, i.e., the capacity between the source and the destination.
- Then, to derive an analytical solution of the capacity, we simplify the model with continuous regions to a model with parallel infinite-length linear source and destination. In this simplified model, the mutual information between the source and the destination is represented by the spatial spectral density (SSD) of the electric field and noise field on the destination. The relationship between the SSD of the current density on the source and the SSD of the electric field on the destination is characterized by the Fourier transform of the Green function. The best current density distribution on the source is then derived based on variational calculus to achieve the maximum mutual information, i.e., the capacity between the source and the destination.
- Furthermore, we consider an improved model of the communication between parallel linear infinite-length source and finite-length destination. By exploiting Mercer expansion, we derive the mutual information between the source and destination. Then we provide an analytical solution of the mutual information, for a given electromagnetic field distribution.
- Finally, we consider a practical model with parallel linear finite-length source and destination. We prove that, the mutual information between the infinite-length source and finite-length destination is an upper bound of that of the finite-length source and destination. Moreover, by exploiting Mercer expansion, we derive the mutual information between the finite-length source and destination.

Organization: The rest of the paper is organized as follows. The communication model based on electromagnetic fields is given in Section II. The spatial correlation analysis of two continuous regions is provided in Section III. For a simplified case of parallel linear source and destination, Section IV provides the mutual information analysis based on SSD. Then, Section V considers a practical model with finite-length destination and derives the mutual information based on Mercer expansion. Finally, conclusions are drawn and future works are discussed in Section VI.

Notation: Bold symbols denote both vectors and matrices; $\mathbb{E}[x]$ denotes the mean of random variable x ; ϵ_0 is the

¹Simulation codes will be provided to reproduce the results presented in this paper: <http://oa.ee.tsinghua.edu.cn/dailinglong/publications/publications.html>.

permittivity of vacuum, μ_0 is the permeability of vacuum, and c is the speed of light in vacuum; $*$ denotes the convolution operation, and $\mathcal{F}[f(x)]$ denotes the Fourier transform of $f(x)$; $(f(x))^+$ is equal to $\frac{f(x)+|f(x)|}{2}$; ∇ is the nabla operator, and $\nabla \times$ is the curl operator; $J_0(x)$ is the Bessel function; $K_0(x)$ is the Bessel function with imaginary argument; $Y_0(x)$ is the Neumann function.

II. ELECTROMAGNETIC WAVE COMMUNICATION MODEL

Maxwell equations, which include four differential equations, reveal that how electromagnetic fields are generated by currents, charges and the change of fields [13]. Here we focus on the latter two equations of Maxwell equations, which are called the Faraday's law and the Ampère's law. The Faraday's law describes how a varying magnetic field generates the electric field, i.e.,

$$\nabla \times \mathbf{E} = -\frac{\partial \mathbf{B}}{\partial t}, \quad (1)$$

and the Ampère's law describes how the current and varying electric field generate the magnetic field, i.e.,

$$\nabla \times \mathbf{H} = \mathbf{J} + \frac{\partial \mathbf{D}}{\partial t}. \quad (2)$$

These equations are the fundamental physical laws that support the electromagnetic wave communications. To simplify the analysis, a common assumption is that, the electromagnetic wave is on a single frequency point, which is the well-known time-harmonic assumption [4]. In this way, the time-frequency part can be separated from the whole expression of the physical quantities of electromagnetic field. For example, the electric field $\mathbf{E}(\mathbf{r}, t)$ can be expressed by $\mathbf{E}(\mathbf{r})e^{-j\omega t}$ under time-harmonic assumption.

Based on the time-harmonic assumption, we can extract the time-frequency item from (1) and (2) to get

$$\nabla \times \mathbf{E} = j\omega \mathbf{B}, \quad (3)$$

and

$$\nabla \times \mathbf{H} = \mathbf{J} - j\omega \mathbf{D}. \quad (4)$$

Perform curl operation on both sides of (3) and substitute (4) into it, we can easily obtain the well-known vector wave equation [14]

$$\nabla \times \nabla \times \mathbf{E}(\mathbf{r}) - \kappa_0^2 \mathbf{E}(\mathbf{r}) = j\omega \mu_0 \mathbf{J}(\mathbf{r}) = j\kappa_0 Z_0 \mathbf{J}(\mathbf{r}), \quad (5)$$

where $\kappa_0 = \omega \sqrt{\mu_0 \epsilon_0}$ is the wavenumber, and $Z_0 = \mu_0 c = 120\pi \Omega$ is the free-space intrinsic impedance.

Consider two arbitrary regions V_t and V_r as the source and the destination for wireless communications. The current density at the source is $\mathbf{J}(\mathbf{r})$, and the induced electric field at the destination is $\mathbf{E}(\mathbf{r})$. The receiving electric field is $\mathbf{Y}(\mathbf{r}) = \mathbf{E}(\mathbf{r}) + \mathbf{N}(\mathbf{r})$, where $\mathbf{N}(\mathbf{r})$ is the noise field. The Green function $\mathbf{G}(\mathbf{r}, \mathbf{s})$ is utilized to solve this equation. Utilizing Green function, the electric field $\mathbf{E}(\mathbf{r})$ can be derived from (5) as

$$\mathbf{E}(\mathbf{r}) = \int_{V_s} \mathbf{G}(\mathbf{r}, \mathbf{s}) \mathbf{J}(\mathbf{s}) d\mathbf{s}, \quad \mathbf{r} \in V_r. \quad (6)$$

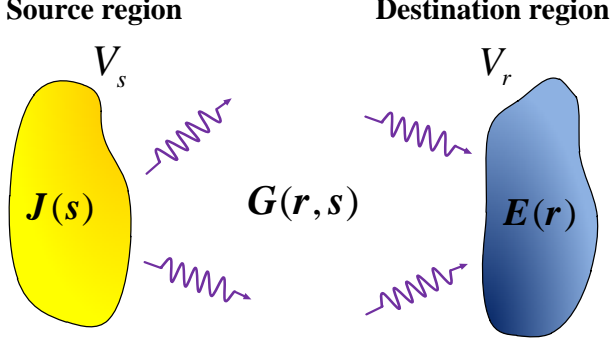


Fig. 1. Electromagnetic model of the communication between two arbitrary continuous regions.

The Green function in unbounded, homogeneous media at fixed frequency point is [15]

$$\begin{aligned} \mathbf{G}(\mathbf{r}, \mathbf{s}) &= -\frac{j\kappa_0 Z_0}{4\pi} \frac{e^{j\kappa_0 \|\mathbf{r}-\mathbf{s}\|}}{\|\mathbf{r}-\mathbf{s}\|} \left(\mathbf{I} + \frac{\nabla_{\mathbf{r}} \nabla_{\mathbf{r}}^H}{\kappa_0^2} \right) \\ &\approx -\frac{j\kappa_0 Z_0}{4\pi} \frac{e^{j\kappa_0 \|\mathbf{r}-\mathbf{s}\|}}{\|\mathbf{r}-\mathbf{s}\|} \left(\mathbf{I} - \hat{\mathbf{p}} \hat{\mathbf{p}}^H \right), \end{aligned} \quad (7)$$

where $\hat{\mathbf{p}} = \frac{\mathbf{p}}{\|\mathbf{p}\|}$ and $\mathbf{p} = \mathbf{r} - \mathbf{s}$.

In this section, the basic model of electromagnetic wave communication has been set up. In the next section, we will use Gaussian random field to capture the statistics of the electromagnetic field, and derive the mutual information by spatial correlation analysis.

III. SPATIAL CORRELATION ANALYSIS OF TWO CONTINUOUS REGIONS

In this section, we provide a method called the spatial correlation analysis to derive the capacity of two continuous regions in electromagnetic fields, as shown in Fig. 1. We use Gaussian random field to characterize the electromagnetic field. The current density $\mathbf{J}(\mathbf{s})$ at the source and the electric field $\mathbf{E}(\mathbf{r})$ at the destination are considered as random fields with autocorrelation function

$$R_{\mathbf{J}}(\mathbf{s}, \mathbf{s}') = \mathbb{E}[\mathbf{J}(\mathbf{s}) \mathbf{J}^H(\mathbf{s}')], \quad (8a)$$

$$R_{\mathbf{E}}(\mathbf{r}, \mathbf{r}') = \mathbb{E}[\mathbf{E}(\mathbf{r}) \mathbf{E}^H(\mathbf{r}')]. \quad (8b)$$

From (6), we can derive the relation between the autocorrelation function of the current density and that of the electric field as

$$\begin{aligned} R_{\mathbf{E}}(\mathbf{r}, \mathbf{r}') &= \mathbb{E}[\mathbf{E}(\mathbf{r}) \mathbf{E}^H(\mathbf{r}')] \\ &= \int_{V_s} \int_{V_s} \mathbf{G}(\mathbf{r}, \mathbf{s}) R_{\mathbf{J}}(\mathbf{s}, \mathbf{s}') \mathbf{G}^H(\mathbf{r}, \mathbf{s}) d\mathbf{s} d\mathbf{s}'. \end{aligned} \quad (9)$$

The noise is modeled as a Gaussian random field with autocorrelation function $R_{\mathbf{N}}(\mathbf{r}, \mathbf{r}')$ [3].

To analyze the amount of mutual information acquired from the electromagnetic field, we introduce sampling on the field. We sample n points on the continuous destination, denoted by $(\mathbf{r}_1, \mathbf{r}_2, \dots, \mathbf{r}_n) = \mathbf{r}_1^n$, where $\mathbf{r}_i \in V_r$, $1 \leq i \leq n$. From

the n three-dimensional spatial sampling points, we obtain $3n$ one-dimensional sampling points. We define

$$\mathbf{E}(r_1^{3n}) = \mathbf{E}(r_1^n) = (\mathbf{E}(\mathbf{r}_1), \mathbf{E}(\mathbf{r}_2), \dots, \mathbf{E}(\mathbf{r}_n)), \quad (10a)$$

$$\mathbf{N}(r_1^{3n}) = \mathbf{N}(r_1^n) = (\mathbf{N}(\mathbf{r}_1), \mathbf{N}(\mathbf{r}_2), \dots, \mathbf{N}(\mathbf{r}_n)). \quad (10b)$$

By considering the noise, the received field at the destination is $\mathbf{Y}(r_1^{3n}) = \mathbf{E}(r_1^{3n}) + \mathbf{N}(r_1^{3n})$. Then, the mutual information between the source and destination over these sampling points is $I(\mathbf{E}(r_1^{3n}); \mathbf{Y}(r_1^{3n}))$, which converges to the mutual information considering the continuous electromagnetic field when n tends to infinity. The capacity C is normalized by the volume of destination V_r as

$$C = \lim_{n \rightarrow \infty} \frac{I(\mathbf{E}(r_1^{3n}); \mathbf{Y}(r_1^{3n}))}{V_r}. \quad (11)$$

The Gaussian random vectors $\mathbf{E}(r_1^{3n})$ and $\mathbf{Y}(r_1^{3n})$ have covariance matrix $\mathbf{K}_E \in \mathbb{C}^{3n \times 3n}$ and $\mathbf{K}_Y \in \mathbb{C}^{3n \times 3n}$. From (7) we know that $\mathbf{G}(\mathbf{r}, \mathbf{s})$ is a function of $\mathbf{r} - \mathbf{s}$, so we can regard (6) as a convolution function with $\mathbf{J}(\mathbf{s}) = 0$ outside V_s . Then, we can derive $\mathbf{J}(\mathbf{s})$ from $\mathbf{E}(\mathbf{r})$ by

$$\mathbf{J}(\mathbf{s}) = \mathcal{F}^{-1} \left[\frac{\mathcal{F}[\mathbf{E}(\mathbf{r})]}{\mathcal{F}[\mathbf{G}(\mathbf{r} - \mathbf{s})]} \right]. \quad (12)$$

Since we can derive $\mathbf{E}(\mathbf{r})$ from $\mathbf{J}(\mathbf{s})$ in (6) and derive $\mathbf{J}(\mathbf{s})$ from $\mathbf{E}(\mathbf{r})$ in (12), we conclude that there is no information loss in the source field conversion. The mutual information between the received signal \mathbf{Y}_1^{3n} and the source signal \mathbf{J}_1^{3n} when n tends to infinity is

$$\begin{aligned} I(\mathbf{Y}_1^{3n}; \mathbf{J}_1^{3n}) &= I(\mathbf{Y}_1^{3n}; \mathbf{E}_1^{3n}) \\ &= h(\mathbf{Y}_1^{3n}) - h(\mathbf{E}_1^{3n} + \mathbf{N}_1^{3n} | \mathbf{E}_1^{3n}) \\ &= h(\mathbf{Y}_1^{3n}) - h(\mathbf{N}_1^{3n}). \end{aligned} \quad (13)$$

The entropy $h(\mathbf{Y}_1^{3n})$ and $h(\mathbf{N}_1^{3n})$ can be derived by the covariance matrix of the Gaussian random vector \mathbf{E} and \mathbf{N}

$$h(\mathbf{Y}_1^{3n}) = \log((\pi e)^{3n} |\mathbf{K}_E + \mathbf{K}_N|), \quad (14a)$$

$$h(\mathbf{N}_1^{3n}) = \log((\pi e)^{3n} |\mathbf{K}_N|). \quad (14b)$$

Then, the mutual information between $\mathbf{Y}(r_1^{3n})$ and $\mathbf{J}(r_1^{3n})$ can be derived as

$$I(\mathbf{Y}_1^{3n}; \mathbf{J}_1^{3n}) = \log \left(\frac{|\mathbf{K}_E + \mathbf{K}_N|}{|\mathbf{K}_N|} \right). \quad (15)$$

The power constraint is expressed as $\frac{1}{n} \text{tr}(\mathbf{K}_E) \leq P_0$. Since $|\mathbf{K}_N|$ is fixed, the maximization of the mutual information $I(\mathbf{Y}_1^{3n}; \mathbf{J}_1^{3n})$ becomes the maximization of $|\mathbf{K}_E + \mathbf{K}_N|$. We perform the similarity diagonalization on \mathbf{K}_N to obtain $\mathbf{K}_N = \mathbf{Q} \Lambda \mathbf{Q}^H$. Then $|\mathbf{K}_E + \mathbf{K}_N|$ can be transformed to

$$\begin{aligned} |\mathbf{K}_E + \mathbf{K}_N| &= |\mathbf{K}_E + \mathbf{Q} \Lambda \mathbf{Q}^H| \\ &= |\mathbf{Q}^H \mathbf{K}_E \mathbf{Q} + \Lambda| \\ &= |\mathbf{A} + \Lambda|. \end{aligned} \quad (16)$$

According to the Kuhn-Tucker conditions, the maximum value is achieved when $A_{ii} = (v - \Lambda_{ii})^+$, where v is chosen to satisfy the power constraint.

In this section, the mutual information between continuous regions is derived in a limit form by spatial correlation

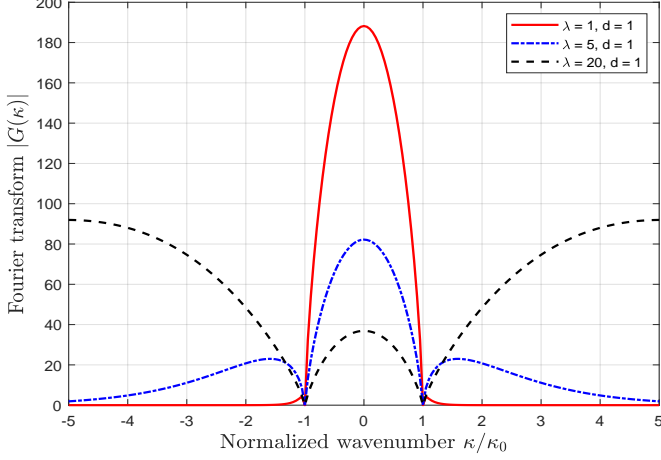


Fig. 2. Fourier transform of the Green function with different wavelengths λ .

analysis. Then, in the next section, we will simplify the model with continuous regions to a new model to obtain an analytical solution of the mutual information.

IV. CAPACITY BETWEEN PARALLEL INFINITE-LENGTH SOURCE AND DESTINATION

In this section, we consider a simplified model with parallel infinite-length linear source and destination. The source is mono polarized to simplify the analysis, which means that the current density has only x direction on the source. For the destination, we only consider the x -direction electric field on it. Thus, in the rest parts of this section, $\mathbf{J}(\mathbf{s})$ and $\mathbf{E}(\mathbf{r})$ have only one dimension. The capacity between the source and destination is defined by the maximum achievable rate on the unit length of them. Similar to the stationary stochastic process in the time domain, we assume that, the current density is also a stationary stochastic process in the space domain. The spatial stationary means that, $\mathbb{E}[J(s)J^*(s')]$ only depends on $\Delta s = s' - s$, and we can introduce the autocorrelation function as

$$R_J(\Delta s) = \mathbb{E}[J(s)J^*(s')]. \quad (17)$$

The SSD can then be derived as

$$S_J(\kappa) = \frac{1}{\sqrt{2\pi}} \int_{-\infty}^{+\infty} R_J(\Delta s) e^{-j\kappa\Delta s} d\Delta s. \quad (18)$$

In our problem setting, we only consider x -dimensional current density and electric field. Therefore, the relationship between $J(s)$ and $E(r)$ can be described using the element in the upper left corner of the matrix \mathbf{G} in (7), which can be derived as

$$g(r, s) = \frac{-jZ_0 e^{j2\pi\sqrt{x^2+d^2}/\lambda}}{2\lambda\sqrt{x^2+d^2}} \left[\frac{d^2}{x^2+d^2} + \frac{j}{2\pi\sqrt{x^2+d^2}/\lambda} \frac{d^2-2x^2}{x^2+d^2} - \frac{1}{(2\pi/\lambda)^2(x^2+d^2)} \frac{d^2-2x^2}{x^2+d^2} \right], \quad (19)$$

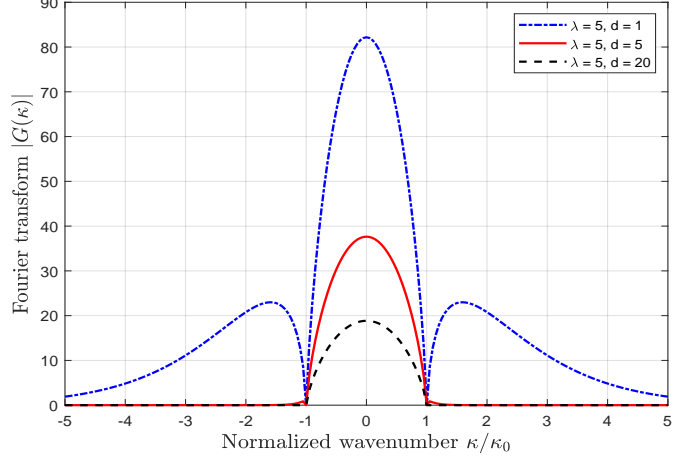


Fig. 3. Fourier transform of the Green function with different distances d .

where $x = r - s$, and d is the distance between the parallel source and destination. Utilizing $g(r, s)$, we can derive

$$E(r) = \int_{-\infty}^{+\infty} g(r, s) J(s) ds, \quad (20)$$

which means that

$$R_E(\Delta r) = \mathbb{E}[E(r)E^*(r')] = \int_{-\infty}^{+\infty} \int_{-\infty}^{+\infty} g(r, s) R_J(\Delta s) g^*(r', s') ds ds'. \quad (21)$$

The SSD of the electric field can then be derived by the SSD of the current density via the Fourier transform of the Green function $G(\kappa)$

$$S_E(\kappa) = 2\pi S_J(\kappa) |G(\kappa)|^2. \quad (22)$$

We introduce **Lemma 1** to derive a closed-form solution for the Fourier transform of the Green function $g(r, s)$.

Lemma 1. *The Fourier transform of the Green function in (19) can be expressed by $G(\kappa) = F_1(\kappa) * F_2(\kappa)$, where*

$$F_1(\kappa) = \frac{-jZ_0 d^2}{4\pi\lambda} \begin{cases} \frac{\pi}{2} j J_0(dm) - \frac{\pi}{2} Y_0(dm), & [0 < \kappa < \frac{2\pi}{\lambda}] \\ K_0(dm), & [\kappa > \frac{2\pi}{\lambda}] \end{cases} \quad (23)$$

with $m = \sqrt{|\left(\frac{2\pi}{\lambda}\right)^2 - \kappa^2|}$, and

$$F_2(\kappa) = d \sqrt{\frac{\pi}{2}} e^{-d|\kappa|} + \frac{jd\lambda}{2\pi} \sqrt{\frac{2}{\pi}} |\kappa| K_1(d|\kappa|) - \frac{j\lambda}{\pi} \left[\sqrt{\frac{2}{\pi}} K_0(d|\kappa|) - d \sqrt{\frac{2}{\pi}} |\kappa| K_1(d|\kappa|) \right] - \left(\frac{\lambda}{2\pi}\right)^2 \frac{1}{2d} \sqrt{\frac{\pi}{2}} (1 + |d\kappa|) e^{-|d\kappa|} + \left(\frac{\lambda}{2\pi}\right)^2 \left[\sqrt{\frac{\pi}{2}} \frac{2e^{-d|\kappa|}}{d} - \frac{1}{d} \sqrt{\frac{\pi}{2}} (1 + |d\kappa|) e^{-|d\kappa|} \right]. \quad (24)$$

Proof: See Appendix A. ■

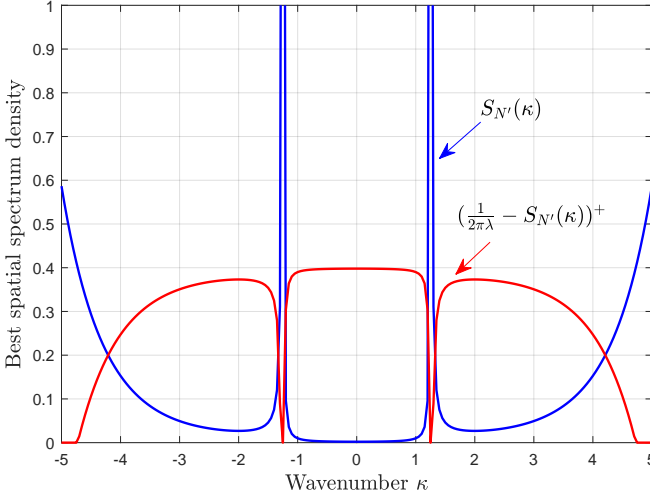


Fig. 4. Best SSD of the current density on the source based on variational calculus.

After deriving the Fourier transform of the Green function in **Lemma 1**, we find that the wavelength λ and the distance between the source and destination d deeply affect the behavior of $|G(\kappa)|$. In Fig. 2 we plot $|G(\kappa)|$ with different wavelengths λ while d is fixed to 1 m. We find that the shape of $|G(\kappa)|$ has a main lobe in $[-\kappa_0, \kappa_0]$. The side lobes vanishes when the wavelength λ decreases below 1 m. Since we have derived $S_E(\kappa) = 2\pi S_J(\kappa)|G(\kappa)|^2$ in (22), when $|G(\kappa)|$ has no side lobe, the SSD of the electric field $S_E(\kappa)$ is band-limited in the wavenumber domain. On the one hand, the DoF of the channel with broad bandwidth in the wavenumber domain is larger than that with narrow one since the DoF outside the band can be exploited, thus increases the channel capacity. On the other hand, the $|G(\kappa)|$ with narrow bandwidth has stronger main lobe, which increases the capacity within $[-\kappa_0, \kappa_0]$. Therefore, we can conclude that when λ changes, the two competing factors, DoF and the gain per degree, decide the tendency of the change of capacity.

In Fig. 3, we plot $|G(\kappa)|$ with different distances d while λ is fixed to 5 m. The side lobe vanishes when the distance d increases above 5 m. We find that, when d decreases, the main lobe and the side lobes both have more energy. Therefore, the DoF and the gain per degree both increase. From this phenomenon, we conclude that with small d which is comparable with the wavelength, we can get more DoFs besides the power gain per degree, thus improving the channel capacity.

From **Lemma 1** we have derived the convolution expression of the Fourier transform of the Green function. Suppose that the noise obeys the spatial additive white Gaussian noise (AWGN) model, which means that the autocorrelation function of the noise $R_N(\Delta s) = \sigma^2 \delta(\Delta s)$ and the SSD of the noise is $S_N(\kappa) = \frac{\sigma^2}{\sqrt{2\pi}}$. Inspired by the integral form of the Shannon capacity for colored AWGN noise channel [16], we assume the power constraint for the source is

$$\int_{-\infty}^{+\infty} S_J(\kappa) d\kappa = P. \quad (25)$$

The channel can be split to infinite narrow-band subchannels in the wavenumber domain. For each of the subchannel, the capacity is

$$C_{\kappa_1} = \frac{1}{2\pi} \log \left(1 + \frac{S_E(\kappa_1)}{S_N(\kappa_1)} \right) d\kappa_1. \quad (26)$$

Therefore, the overall capacity is

$$\begin{aligned} C &= \frac{1}{2\pi} \int_{-\infty}^{+\infty} \log \left(1 + \frac{S_E(\kappa)}{S_N(\kappa)} \right) d\kappa \\ &= \frac{1}{2\pi} \int_{-\infty}^{+\infty} \log \left(1 + \frac{2\pi S_J(\kappa)}{S_N(\kappa)/|G(\kappa)|^2} \right) d\kappa. \end{aligned} \quad (27)$$

To simplify the analysis, we introduce the equivalent noise N' with SSD $S_{N'}(\kappa) = S_N(\kappa)/(2\pi|G(\kappa)|^2)$. To derive the best SSD of the current density $S_J(\kappa)$, we obtain the following **Theorem 1**.

Theorem 1. *For the overall capacity in (27) and the power constraint for the current density in (25), the SSD of the best current density obeys $S_J(\kappa) = (\frac{1}{2\pi\lambda} - S_{N'}(\kappa))^+$, where λ is obtained by the power constraint.*

Proof: In order to obtain the optimal SSD $S_J(\kappa)$ that maximizes (27), we apply the variational calculus. The Lagrange multiplier λ can be introduced to take into consideration the power constraint $\int S_J d\kappa \leq P_J$:

$$\begin{aligned} \mathcal{L}(S_J, \lambda) &= \frac{1}{2\pi} \int_{-\infty}^{+\infty} \log \left(1 + \frac{S_J(\kappa)}{S_{N'}(\kappa)} \right) d\kappa \\ &\quad - \lambda \left(\int_{-\infty}^{+\infty} S_J(\kappa) d\kappa - P_J \right). \end{aligned} \quad (28)$$

Taking the variation of (28), we obtain

$$\delta C = \frac{1}{2\pi} \int_{-\infty}^{+\infty} \frac{1}{1 + \frac{S_J(\kappa)}{S_{N'}(\kappa)}} \frac{\delta S_J(\kappa)}{S_{N'}(\kappa)} d\kappa - \lambda \int_{-\infty}^{+\infty} \delta S_J(\kappa) d\kappa. \quad (29)$$

From (29), we can find that the optimal solution for S_J should satisfy

$$\frac{1}{2\pi(S_J(\kappa) + S_{N'}(\kappa))} - \lambda \equiv 0. \quad (30)$$

Taking the non-negative condition on S_J into consideration, we obtain

$$S_J(\kappa) = \left(\frac{1}{2\pi\lambda} - S_{N'}(\kappa) \right)^+. \quad (31)$$

For example, when the wavelength λ is 5 m and the distance d between the two parallel lines is 1 m, the Fourier transform of the Green function is shown in Fig. 3. We use AWGN model with the noise SSD $S_N(\kappa) = 90$. The power constraint for the current density P is equal to 3. From (31) we can derive the best SSD of the source current, as shown in Fig. 4. ■

In this section, we have derived the capacity between parallel infinite-length linear source and destination. For a more practical model, in the next section, we will focus on scenario with finite-length destination.

V. CAPACITY WITH FINITE-LENGTH DESTINATION

In this section, we consider the communication between parallel linear source and destination when the length of the destination is finite. In Subsection V-A, we develop the model with finite-length source and infinite-length source, separately. Then in Subsection V-B, we prove that, the mutual information between the infinite-length source and the destination is an upper bound of that of the finite-length source and destination. Finally, in Subsection V-C, we use Mercer Expansion to derive the mutual information of these two cases, and an analytical solution is also provided for a given electric field.

A. System Model

We assume that the linear source and destination are parallel and the distance between them is d . The destination has finite length. Both the infinite-length source and the length- L source are considered respectively, as follows.

1) *System model with infinite-length source*: We denote the autocorrelation function on the source as $R_J(s, s')$, $s, s' \in (-\infty, +\infty)$. The current density J is modeled as a spatial stationary stochastic process as in Section IV. The electric field E on the receiver is also a spatial stationary stochastic process.

2) *System model with finite-length source*: We denote the autocorrelation function on the source as $R_J(s, s')$, $s, s' \in [-L/2, +L/2]$. The current density J has arbitrary distribution and may not be spatial stationary.

B. Relationship between the Two Cases

In this subsection, we begin from the model with finite-length source and destination. Then, by using the stationarization method, we find its relationship with the model which has infinite-length source and spatial stationary current density. In the extension procedure, we prove that, the mutual information between the infinite-length source and finite-length destination is an upper bound of that of the finite-length source and destination.

If we consider the finite-length linear source as a line segment, we can easily get an virtual infinite-length line, which is the extension of the finite source. The virtual line can be split into infinite length- L parts, and the original source is placed in one part. The autocorrelation function of the current density on the original source is copied to all length- L parts. Moreover, the current densities in different parts are noncoherent. Now we construct a periodically nonstationary process $J'(s)$ on the virtual line, which means that the joint distributions of $J'(s)$ are invariant under spatial shifts of length L . Now the autocorrelation function of the current density on the virtual line becomes

$$R_{J'}(s, s') = \begin{cases} R_J(s - n_1 L, s' - n_2 L), & n_1 = n_2 \\ 0, & n_1 \neq n_2 \end{cases} \quad (32)$$

where $s \in [-L/2 + n_1 L, L/2 + n_1 L]$, $s' \in [-L/2 + n_2 L, L/2 + n_2 L]$ and $n_1, n_2 \in \mathbb{Z}$.

After constructing $J'(s)$, we now operate random shift on $J'(s)$ to construct a spatial stationary stochastic process $J''(s) = J'(s + \theta)$ [17]. The random shift means to add a

random spatial phase factor θ to $J'(s)$, where θ is uniformly distributed within $[0, L]$. To extend the random shift in [17], we obtain the following **Lemma 2**.

Lemma 2. *Suppose we have a periodically nonstationary process $J'(s)$ which has period L . Then we operate random shift θ' on $J'(s)$, where θ' is uniformly distributed on $[x, x+L]$, x is an arbitrary real number. The constructed stochastic process $J'''(s) = J'(s + \theta')$ is a spatial stationary stochastic process.*

Proof: We already know from [17] that $J''(s) = J'(s + \theta)$ is spatial stationary when θ is uniformly distributed on $[0, L]$. Since $J'''(s) = J''(s + x)$, it is obvious that $J'''(s)$ is also spatial stationary. ■

To derive the correlation between the capacity with infinite-length source and that with finite-length source, we obtain the following **Theorem 2**.

Theorem 2. *Define $I_{L,L}$ as the capacity between parallel length- L linear source and destination. The current density on the source is $J(s)$. Define $I_{\infty,2L}$ as the capacity between an infinite-length source with current density $J''(s)$ and the parallel length- $2L$ destination. If $J''(s)$ is a stationary process constructed from $J(s)$ by the stationarization method mentioned above, $I_{L,L} \leq I_{\infty,2L}$ holds for arbitrary current density $J(s)$ on the source.*

Proof: See Appendix B. ■

Remark 1: From **Theorem 2**, we can derive the upper bound of the capacity of the communication system between finite length source and destination with non-stationary stochastic process. The upper bound is the capacity between an infinite-length source with a stationary stochastic process and a length- $2L$ receiver. The capacity with a spatial stationary stochastic process is easier to analyze, while that with a non-stationary process is more general and useful. The lower bound remains to be explored.

In this subsection we have derived the relationship between the two cases with infinite-length source and finite-length source. In the next section, we will build a closed-form formula for the mutual information of these two cases using the Mercer Expansion.

C. Capacity Solution Based on Mercer Expansion

In Section III, we have derived the mutual information between source and destination with spatial stationary electromagnetic field. In this section, for finite-length destination, the spatial stationary assumption does not hold. To derive the mutual information in this scenario, we use Mercer Expansion [18] to expand the received electric field on a series of orthogonal basis.

For the case when the source is infinite, the current density is $J''(s)$ and the autocorrelation function of the current density is $R_{J''}(s, s')$. From (21), we can derive the autocorrelation function of the electric field as

$$R_E(r, r') = \int_{-\infty}^{+\infty} \int_{-\infty}^{+\infty} g(r, s) R_{J''}(s, s') g^*(r', s') ds ds'. \quad (33)$$

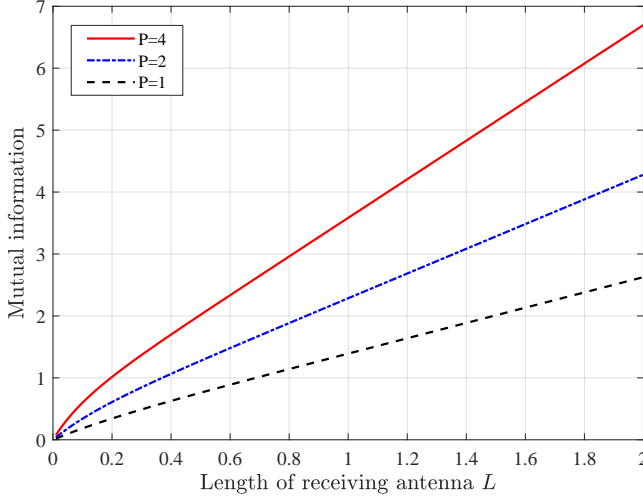


Fig. 5. Mutual information $I(L)$ calculated by the Mercer Expansion.

For the case when the source has finite length, we assume the current density on the source is $J(s)$ and its autocorrelation function is $R_J(s, s')$, where $s, s' \in [0, L]$. The electric field on the receiver is

$$E(r) = \int_0^L g(r, s) J(s) ds. \quad (34)$$

The autocorrelation function of the receiving electric field is

$$\begin{aligned} R_E(r, r') &= \mathbb{E} \left[\int_0^L g(r, s) J(s) ds \int_0^L g(r', s') J(s') ds' \right] \\ &= \mathbb{E} \left[\int_0^L \int_0^L g(r, s) J(s) J(s') g(r', s') ds ds' \right] \\ &= \int_0^L \int_0^L g(r, s) R_J(s, s') g^*(r', s') ds ds'. \end{aligned} \quad (35)$$

The Mercer Expansion of the electric field is

$$R_E(r, r') = \sum_{k=1}^{+\infty} \lambda_k \phi_k(r) \phi_k(r'), \quad (36)$$

where $\phi_k(r)$ is the solution of the integral function

$$\lambda_k \phi_k(r') = \int_0^L R_E(r, r') \phi_k(r) dr; k > 0, k \in \mathbb{N}. \quad (37)$$

The eigenfunctions are orthogonal

$$\int_0^L \phi_{k_1}(r) \phi_{k_2}(r) dr = \delta_{k_1 k_2}. \quad (38)$$

For the noise field, the Mercer Expansion also exists and we denote the eigenfunctions by $\phi'_k(r)$ and the eigenvalues by λ'_k .

We consider the scenario where the receiver is finite and the noise field is white Gaussian noise with the noise power spectral density assumed to be $n_0/(2\sqrt{2\pi})$. The Gaussian white noise has the autocorrelation function $R_N(r, r') = \frac{n_0}{2} \delta(r - r')$, which means that for any function $\phi_k(r)$, the integral function

$$\frac{n_0}{2} \phi_k(r') = \int_0^L R_N(r, r') \phi_k(r) dr; k > 0, k \in \mathbb{N}. \quad (39)$$

holds. Therefore, the received electric field and the noise can be expanded on the same orthogonal bases $\phi_k(r)$, and the mutual information between the source and destination can be expressed by the eigenvalues as follows

$$I = \sum_{k=1}^{+\infty} \log \left(1 + \frac{\lambda_k}{n_0/2} \right). \quad (40)$$

Rigorous proof is similar to **Theorem 1** in [19].

To derive an analytical solution of the capacity, we consider a special case when the autocorrelation function of the electric field is $R_E(r, r') = Pe^{-\alpha|r-r'|}$. The solution for the integral function (37) is

$$\lambda_k = \frac{2\alpha P}{\alpha^2 + \omega_k^2}, \quad (41a)$$

$$\phi_k(r) = \frac{1}{Z_k} (\omega_k \cos(\omega_k r) + \alpha \sin(\omega_k r)), \quad (41b)$$

where Z_k are the normalization constraints to ensure the orthogonality in (38) and ω_k is the solution of

$$2\arctan(\omega_k/\alpha) = k\pi - \omega_k T. \quad (42)$$

In Fig. 5, we plot the mutual information derived by the Mercer Expansion according to (40). Our results show that, the mutual information increases linearly with the length of receiver L when L is large enough. When L tends to infinity, the mutual information normalized by length will tends to the mutual information derived in Section III.

VI. CONCLUSIONS

In this paper, we analyzed the capacity of electromagnetic fields based on spatial correlation analysis. We first developed the system model of the communication between two four-dimensional continuous regions based on random field. The model based on random field provided a general framework for solving the problems like capacity for EIT. Then, we considered a simplified model with parallel infinite-length linear source and destination and analyzed the mutual information by SSD. During this procedure, we showed the high DoF contained in the electromagnetic near field by the Fourier transform of the Green function. Finally, we considered the practical model with finite-length destination and used Mercer expansion to derive the mutual information. The capacity we analyzed revealed the ultimate performance limit of two continuous regions, which can provide guidance for practical communication systems.

Future works may be explored on the analytical solutions of more general cases like non-linear source and destination. The correlation between the current density distribution on the source and the radiated power in the space is also necessary to be investigated.

APPENDIX A

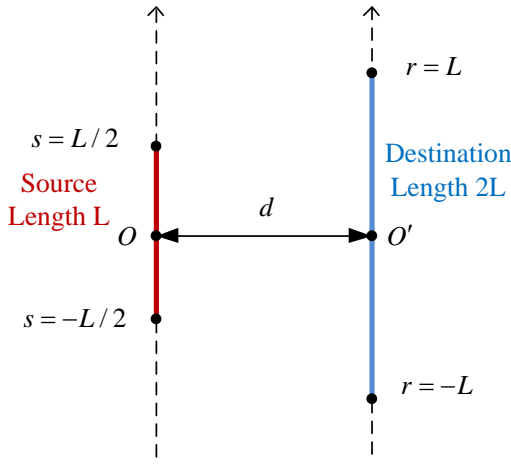


Fig. 6. Parallel linear source and destination.

PROOF OF LEMMA 1

For the Green function in (19), we split it into the product of two functions $g(x) = f_1(x)f_2(x)$, where

$$f_1(x) = \frac{-jZ_0\eta e^{j2\pi\sqrt{x^2+d^2}/\lambda}}{2\lambda\sqrt{x^2+d^2}}, \quad (43a)$$

$$f_2(x) = \left[\frac{d^2}{x^2+d^2} + \frac{j}{2\pi\sqrt{x^2+d^2}/\lambda} \frac{d^2-2x^2}{x^2+d^2} \right. \quad (43b) \\ \left. - \frac{1}{(2\pi/\lambda)^2(x^2+d^2)} \frac{d^2-2x^2}{x^2+d^2} \right].$$

Utilizing the convolution theory, we can express $G(\kappa)$ by $G(\kappa) = F_1(\kappa) * F_2(\kappa)$, where $F_1(\kappa) = \mathcal{F}[f_1(x)]$ and $F_2(\kappa) = \mathcal{F}[f_2(x)]$. For the Fourier transform of $f_1(x)$, we have

$$F_1(\kappa) = \frac{1}{\sqrt{2\pi}} \int_{-\infty}^{+\infty} \frac{-jZ_0 e^{j2\pi\sqrt{x^2+d^2}/\lambda}}{2\lambda\sqrt{x^2+d^2}} e^{j\kappa x} dx \quad (44) \\ = A_1 + A_2,$$

where

$$A_1 = \frac{1}{\sqrt{2\pi}} \int_{-\infty}^{+\infty} \frac{-jZ_0 e^{j2\pi\sqrt{x^2+d^2}/\lambda}}{2\lambda\sqrt{x^2+d^2}} \cos\kappa x dx, \quad (45)$$

and

$$A_2 = \frac{1}{\sqrt{2\pi}} \int_{-\infty}^{+\infty} \frac{Z_0 e^{j2\pi\sqrt{x^2+d^2}/\lambda}}{2\lambda\sqrt{x^2+d^2}} \sin\kappa x dx. \quad (46)$$

Since $\frac{Z_0 e^{j2\pi\sqrt{x^2+d^2}/\lambda}}{2\lambda\sqrt{x^2+d^2}}$ is an even function, it is obvious that A_2 equals 0. For A_1 , we utilize [20, Eq. (3.876)] to get

$$A_1 = \frac{-jZ_0 d^2}{4\pi\lambda} \begin{cases} \frac{\pi}{2} j J_0(dm) - \frac{\pi}{2} Y_0(dm), & [0 < |\kappa| < \frac{2\pi}{\lambda}] \\ K_0(dm), & [|\kappa| > \frac{2\pi}{\lambda}] \end{cases} \quad (47)$$

where m denotes $\sqrt{\left(\frac{2\pi}{\lambda}\right)^2 - \kappa^2}$. Then we obtain the closed-form solution of $F_1(\kappa) = A_1$.

For the Fourier transform of $f_2(x)$, we need to derive the Fourier transform of $\frac{1}{(d^2+x^2)^{3/2}}$, $\frac{x^2}{(d^2+x^2)^{3/2}}$, $\frac{1}{(d^2+x^2)^2}$ and $\frac{x^2}{(d^2+x^2)^2}$. From [20, Eq. (3.961)], we can get

$$\mathcal{F}\left[\frac{1}{(d^2+x^2)^{3/2}}\right] = \frac{1}{d} \sqrt{\frac{2}{\pi}} |\kappa| K_1(d|\kappa|), \quad (48)$$

$$\mathcal{F}\left[\frac{x^2}{(d^2+x^2)^{3/2}}\right] = \sqrt{\frac{2}{\pi}} K_0(d|\kappa|) - d \sqrt{\frac{2}{\pi}} |\kappa| K_1(d|\kappa|). \quad (49)$$

For $\frac{1}{(d^2+x^2)^2}$, we use residue theorem to get

$$\mathcal{F}\left[\frac{1}{(d^2+x^2)^2}\right] = 2\pi j \operatorname{Res}_{x=jd} \left[\frac{e^{j\kappa x}}{(d^2+x^2)^2} \right] \quad (50) \\ = \frac{1}{2d^3} \sqrt{\frac{\pi}{2}} (1 + |d\kappa|) e^{-|d\kappa|}.$$

For $\frac{x^2}{(d^2+x^2)^2}$, we can get

$$\mathcal{F}\left[\frac{x^2}{(d^2+x^2)^2}\right] = \mathcal{F}\left[\frac{1}{d^2+x^2}\right] - d^2 \mathcal{F}\left[\frac{1}{(d^2+x^2)^2}\right] \\ = \frac{\sqrt{\frac{\pi}{2}} e^{-d|\kappa|}}{d} - \frac{1}{2d} \sqrt{\frac{\pi}{2}} (1 + |d\kappa|) e^{-|d\kappa|} \quad (51)$$

Finally, we can get

$$F_2(\kappa) = d \sqrt{\frac{\pi}{2}} e^{-d|\kappa|} + \frac{j\lambda}{2\pi} \sqrt{\frac{2}{\pi}} |\kappa| K_1(d|\kappa|) \\ - \frac{j\lambda}{\pi} \left[\sqrt{\frac{2}{\pi}} K_0(d|\kappa|) - d \sqrt{\frac{2}{\pi}} |\kappa| K_1(d|\kappa|) \right] \\ - \left(\frac{\lambda}{2\pi} \right)^2 \frac{1}{2d} \sqrt{\frac{\pi}{2}} (1 + |d\kappa|) e^{-|d\kappa|} \\ + \left(\frac{\lambda}{2\pi} \right)^2 \left[\sqrt{\frac{\pi}{2}} \frac{2e^{-d|\kappa|}}{d} - \frac{1}{d} \sqrt{\frac{\pi}{2}} (1 + |d\kappa|) e^{-|d\kappa|} \right]. \quad (52)$$

APPENDIX B PROOF OF THEOREM 2

To prove that $I_{L,L} \leq I_{\infty,2L}$, we introduce an intermediate variable $I_{L,2L}$, which denotes the capacity between a length- L source and a length- $2L$ source. The source and destination are parallel and the distance between them is d . The relative position of the source and destination is shown in Fig. 6. Two independent one-dimensional axes are used to mark the positions of the source and destination. The connecting line OO' of the two origins is perpendicular to the source and destination. To denote the position of the source and destination, we use the coordinate of the lowest point on them. For example, the position of the source which covers $[-L/2, L/2]$ is denoted by $s = -L/2$.

In the following proof, we split the original problem into two inequalities $I_{L,L} \leq I_{L,2L}$ and $I_{L,2L} \leq I_{\infty,2L}$ and verify them separately.

The first inequality is obvious because the source current density converses and the length- $2L$ receiver covers the length- L destination. The mutual information with a larger receiver

should be no less than the mutual information with a smaller destination.

For the second inequality, we fix the position of the destination and shift the source along the virtual line. We denote the mutual information between the source and destination with respect to the position of the source s as $I(s)$. It is obvious that, when s varies from $-L$ to 0, there exists $s = s_0$ which achieves the minimum mutual information $I_{L,2L}(s_0)$. When the receiver is shortened to a length- L line located at s_0 , the mutual information is exactly $I_{L,L}$. Therefore, we conclude that $I_{L,2L}(s_0) \geq I_{L,L}$ and

$$I_{L,2L}(s) \geq I_{L,L}, \forall s \in [-L, 0]. \quad (53)$$

From **Lemma 1** we note that, the procedure of turning $J(s)$ on the length- L source to the spatial stationary stochastic process $J''(s)$ on the infinite length source contains two steps²:

- 1) the spatial copy and 2) the spatial random shift θ' .

Therefore, in our proof we first operate the spatial random shift θ' on $J(s)$, resulting in a new current density $J(s + \theta')$. From (53) we can get

$$\mathbb{E}[I_{L,2L}(s)] \geq I_{L,L}, \quad (54)$$

which means that the random shift operation does not decrease the mutual information.

Secondly, we perform the spatial copy operation on the shifted source. We denote the current density on the shifted source by J_1 and the copied current densities by J_i , $2 \leq i \leq \infty$. These current densities have the same distribution but are mutually independent. The electric field generated by these current densities are denoted by E_i , $1 \leq i \leq \infty$. The total received field is

$$E_{\text{total}} = \sum_{i=1}^{+\infty} E_i + N, \quad (55)$$

where N is the noise field.

To complete the proof, we only need to show that $I(E_{\text{total}}; J_1 \dots J_n) \geq I(E_{\text{single}}; J_1)$ for arbitrary n , where $E_{\text{single}} = E_1 + N$ is the received field without the spatial copy operation. Since

$$\begin{aligned} I(E_{\text{total}}; J_1 \dots J_n) &= h(E_{\text{total}}) - h(E_{\text{total}}|J_1 \dots J_n) \\ &= h(E_{\text{total}}) - h(N), \end{aligned} \quad (56)$$

and

$$\begin{aligned} I(E_{\text{single}}; J_1) &= h(E_{\text{single}}) - h(E_{\text{single}}|J_1) \\ &= h(E_{\text{single}}) - h(N), \end{aligned} \quad (57)$$

we only need to prove that $h(E_{\text{total}}) \geq h(E_{\text{single}})$, which equals to prove $h(X + Y) \geq h(X)$ when X and Y are independent. We have

$$\begin{aligned} h(X + Y, Y) &= h(X + Y|Y) + h(Y) \\ &= h(X|Y) + h(Y) \\ &= h(X, Y), \end{aligned} \quad (58)$$

and

$$h(X + Y, Y) = h(Y|X + Y) + h(X + Y). \quad (59)$$

²Exchanging the order of these two steps does not affect the result.

Then we can get

$$\begin{aligned} h(X + Y) &= h(X, Y) - h(Y|X + Y) \\ &= h(X) + I(Y; X + Y) \\ &\geq h(X), \end{aligned} \quad (60)$$

which completes the proof of **Theorem 2**.

REFERENCES

- [1] C. E. Shannon, "A mathematical theory of communication," *The Bell system technical journal*, vol. 27, no. 3, pp. 379–423, Jul. 1948.
- [2] A. Kaye and D. George, "Transmission of multiplexed PAM signals over multiple channel and diversity systems," *IEEE Trans. Commun. Technol.*, vol. 18, no. 5, pp. 520–526, Oct. 1970.
- [3] L. Sanguinetti, A. A. D'Amico, and M. Debbah, "Wavenumber-division multiplexing in line-of-sight holographic MIMO communications," *arXiv preprint arXiv:2106.12531*, Jun. 2021.
- [4] F. K. Gruber and E. A. Marengo, "New aspects of electromagnetic information theory for wireless and antenna systems," *IEEE Trans. Antennas Propag.*, vol. 56, no. 11, pp. 3470–3484, Nov. 2008.
- [5] M. D. Migliore, "Horse (electromagnetics) is more important than horseman (information) for wireless transmission," *IEEE Trans. Antennas Propag.*, vol. 67, no. 4, pp. 2046–2055, Apr. 2018.
- [6] O. Bucci, G. Franceschetti, and G. d'Elia, "Fast analysis of large antennas—a new computational philosophy," *IEEE Trans. Antennas Propag.*, vol. 28, no. 3, pp. 306–310, Dec. 1980.
- [7] D. Slepian, "On bandwidth," *Proc. of the IEEE*, vol. 64, no. 3, pp. 292–300, Mar. 1976.
- [8] A. V. Balakrishnan, "A note on the sampling principle for continuous signals," *IRE Trans. Inf. Theory*, vol. 3, no. 2, pp. 143–146, Jun. 1957.
- [9] O. Bucci and G. Franceschetti, "On the spatial bandwidth of scattered fields," *IEEE Trans. Antennas Propag.*, vol. 35, no. 12, pp. 1445–1455, Dec. 1987.
- [10] M. Franceschetti, "On Landau's eigenvalue theorem and information cut-sets," *IEEE Trans. Inf. Theory*, vol. 61, no. 9, pp. 5042–5051, Jul. 2015.
- [11] N. Decarli and D. Dardari, "Communication modes with large intelligent surfaces in the near field," *arXiv preprint arXiv:2108.10569*, Aug. 2021.
- [12] Z. Zhang and L. Dai, "Continuous-aperture MIMO for electromagnetic information theory," *arXiv preprint arXiv:2111.08630*, Nov. 2021.
- [13] D. J. Griffiths, *Introduction to electrodynamics*. American Association of Physics Teachers, 2005.
- [14] D. Dardari, "Communicating with large intelligent surfaces: Fundamental limits and models," *IEEE J. Sel. Areas Commun.*, vol. 38, no. 11, pp. 2526–2537, Nov. 2020.
- [15] A. S. Poon, R. W. Brodersen, and D. N. Tse, "Degrees of freedom in multiple-antenna channels: A signal space approach," *IEEE Trans. Inf. Theory*, vol. 51, no. 2, pp. 523–536, Jan. 2005.
- [16] C. E. Shannon, "Communication in the presence of noise," *Proc. of the IRE*, vol. 37, no. 1, pp. 10–21, Jan. 1949.
- [17] H. Hurd, "Stationarizing properties of random shifts," *SIAM Journal on Applied Mathematics*, vol. 26, no. 1, pp. 203–212, Jan. 1974.
- [18] J. Mercer, "Functions of positive and negative type, and their connection with the theory of integral equations," *Philos. Trans. Roy. Soc. London*, vol. 209, no. 441–458, pp. 415–446, Jan. 1909.
- [19] J. Zhu, Z. Zhang, Z. Wan, and L. Dai, "Finite-time capacity: Making exceed-shannon possible?" *arXiv preprint arXiv:2111.00444*, Nov. 2021.
- [20] D. Zwillinger, V. Moll, I. Gradshteyn, and I. Ryzhik, Eds., *Table of Integrals, Series, and Products (Eighth Edition)*. Boston: Academic Press, 2014.